Inclusion of a Drag Approach in the Town Energy Balance (TEB) Scheme: Offline 1D Evaluation in a Street Canyon

R. HAMDI

Royal Meteorological Institute, Brussels, Belgium

V. MASSON

Centre National de Recherches Météorologiques, Toulouse, France

ABSTRACT

The Town Energy Balance module bridges the micro- and mesoscale and simulates local-scale urban surface energy balance for use in mesoscale meteorological models. Previous offline evaluations show that this urban module is able to simulate in good behavior road, wall, and roof temperatures and to correctly partition radiation forcing into turbulent and storage heat fluxes. However, to improve prediction of the meteorological fields inside the street canyon, a new version has been developed, following the methodology described in a companion paper by Masson and Seity. It resolves the surface boundary layer inside and above urban canopy by introducing a drag force approach to account for the vertical effects of buildings. This new version is tested offline, with one-dimensional simulation, in a street canyon using atmospheric and radiation data recorded at the top of a 30-m-high tower as the upper boundary conditions. Results are compared with simulations using the original single-layer version of the Town Energy Balance module on one hand and with measurements within and above a street canyon on the other hand. Measurements were obtained during the intensive observation period of the Basel Urban Boundary Layer Experiment. Results show that this new version produces profiles of wind speed, friction velocity, turbulent kinetic energy, turbulent heat flux, and potential temperature that are more consistent with observations than with the single-layer version. Furthermore, this new version can still be easily coupled to mesoscale meteorological models.

1. Introduction

Mesoscale meteorological models (MMMs) are often modified to simulate and eventually to forecast urban climate phenomena such as urban heat islands and city-induced circulations in the atmospheric boundary layer (Kusaka et al. 2001; Lemonsu and Masson 2002; Dupont et al. 2004; Otte et al. 2004; Roulet et al. 2005; Dandou et al. 2005; Hamdi 2005; Best 2005, 2006; Holt and Pullen 2007; the COST Action 715, Piringer et al. 2007; FUMAPEX project, Baklanov et al. 2006). To modify these MMMs, numerous modules that simulate the surface energy balance of the urban canopy are described in the literature (e.g., Masson 2000; Grim-

mond and Oke 2002; Martilli et al. 2002; Dupont and Mestayer 2006), and according to Masson (2006), they can be classified into three main categories.

(i) Empirical modules: These modules are based on observations of surface energy balance and the objective is to reproduce the energetics of urban canopy using statistical relations derived from observations. One of the more accurate of these schemes is the Local-Scale Urban Meteorological Preprocessing Scheme of Grimmond and Oke (2002). It computes the energy balance with semiempirical parameterizations, including the Objective Hysteresis Model (Grimmond and Oke 1999). This type of approach makes it possible to use extremely simple schemes. The main weakness, however, is that the statistics are limited to land cover characteristics and to climatic and seasonal conditions encountered in the original studies.

Corresponding author address: R. Hamdi, Royal Meteorological Institute, Avenue Circulaire, 3, B-1180 Brussels, Belgium.
E-mail: rafiq.hamdi@oma.be

(ii) Modified vegetation schemes: The advantage is that for soil–vegetation–atmosphere transfer (SVAT) schemes a large background literature is available (Brown 2000). However, modifications are necessary to take into account thermal and dynamical effects of the urban canopy:

1) With respect to the dynamical properties of urban surfaces, two main approaches exist. One consists in applying roughness classification or morphometric schemes (Grimmond and Oke 1999, 2002) based on the observation that roughness length and displacement height are large over cities. These surface schemes are forced by only one atmospheric layer (the lowest layer of an MMM). Note that this level is physically supposed to be high enough above the surface to be in the inertial sublayer (or constant flux layer) where most schemes use the Monin–Obukhov theory to parameterize turbulent fluxes. Alternatively, with the so-called drag force approach, a term is added to momentum and turbulent kinetic energy (TKE) equations to account for obstacle drag, as used in the models of Brown (2000) or Dupont et al. (2004). The main disadvantage of drag-based schemes is that they imply directly modifying the equations of the MMMs to which they are coupled.

2) With respect to the thermal properties, energy balance is often modified to take into account radiation trapping in the urban canopy, heat storage term, evaporation, and anthropogenic heat fluxes.

(iii) Urban canopy modules: These modules are exclusively urban, fitted to the structure of regular dense city centers. They are based on a 3D shape of buildings, they solve separate energy balances for roof, road, and wall, and the radiative interactions between road and wall are explicitly treated. One of the benefits of using distinct surface types is that their properties are more easily interpreted than the corresponding averaged quantities found in modified vegetation schemes. However, except for some schemes that include vegetation in the street, for mostly urban canopy modules, neither sparse vegetation nor empty areas are allowed in the urban canyon. Therefore, for simulating large areas they must be associated with a rural soil module to compute the transfers at natural surfaces. A tiling approach is then used to represent the heterogeneity of real urban areas, with the disadvantage that the two modules do not exchange with each other at the subgrid scale (Dupont and Mestayer 2006). As for modified vegetation schemes, urban canopy modules can be separated into two main categories: those where canopy air is parameterized and all urban effects are considered to be subgrid scale in the vertical (this category is referred to as single-layer modules); the second category is called multilayer modules in that urban effects are computed vertically throughout the urban canopy.

The urban parameterization scheme of Martilli et al. (2002), is a recent example of multilayer urban modules. This scheme presents a high level of detail of the surface energy balance, since it gives users the maximum of freedom in choosing urban parameters (road orientations, building heights, etc.) for each urban class. Note that each urban grid cell can be presented as a combination of several urban classes. This scheme solves a separate energy balance at each air level inside the street canyon and computes the impact of every urban surface type (roads, roofs, and walls) on momentum, heat, and TKE equations separately; these additional terms are taken into account in proportion to their respective fractions. This scheme also considers shadowing and radiation trapping effects, adapts turbulent length scales, and introduces an anthropogenic heat source by fixing the internal temperature of walls. Martilli's urban module has been successfully tested against observations in Basel (Switzerland) city center in Roulet et al. (2005) and Hamdi and Schayes (2005). However, because of the detail of this scheme, computational cost is relatively high.

In the Town Energy Balance (TEB; Masson 2000) single-layer module, urban canopy is assumed to be an isotropic array of street canyons. The advantage is that relatively few individual surface energy balance evaluations need to be resolved, radiation interactions are simplified, and therefore computational time is kept low. TEB simulates heat and water exchanges and climate of three generic surfaces (roof, wall, and road), where heat transfers are computed through several layers of materials, generally four. Anthropogenic heat and vapor releases from buildings, vehicles, and chimneys can also be added. This module is essentially designed to provide canopy heat fluxes for the lower boundary condition of MMMs. It can be run on its own for highly urbanized sites. For areas that include vegetated tiles, Noilhan and Planton's (1989) Interaction between Soil, Biosphere, and Atmosphere (ISBA) scheme can be added. TEB is forced with literature-based surface thermal parameters and observed or simulated atmospheric and radiation data from above roof level. Despite the simplification hypotheses, offline simulations of TEB have been shown to accurately

reproduce surface energy balance, canyon air temperature, and surface temperatures observed in dense urban areas (Masson et al. 2002; Lemonsu et al. 2004). However, since TEB is a single-layer module, then characteristics of air inside the canyon space must be specified. In fact, the logarithmic law for wind is assumed to apply down to the layer around roof top, and an exponential decay law is used below (Cionco 1965; Macdonald 2000). Air temperature and humidity are assumed to be uniform inside the street canyon (Masson 2000). So, to improve meteorological field prediction inside the street canyon, a new version of TEB has been developed. It resolves the surface boundary layer (SBL) inside and above urban canopy by including a drag force approach to account for the vertical effects of buildings as is done in Martilli's parameterization except that only one surface energy balance per wall is resolved. Thus, calculation of heat fluxes is not required at each level inside the urban canopy. Two other models of this type have been developed, one by Vu et al. (1999, 2002) and the other by Kondo and Liu (1998).

Therefore, the goal of the present contribution is (i) to include an SBL scheme as well as a drag approach in the TEB scheme, using the general methodology described in Masson and Seity (2008, manuscript submitted to *J. Appl. Meteor. Climatol.*), (ii) to validate it with measurements obtained within and above a street canyon, and (iii) to do a comparison between the Lemonsu et al. (2004) version of TEB and this simplified multilayer version, since there are currently few reports about comparisons between single and multilayer urban modules (e.g., Kusaka et al. 2001; Holt and Pullen 2007).

In this paper, we discuss the formulation and implementation of the drag approach in TEB in section 2. Section 3 contains a description of the real-data case used to validate this new version of TEB and simulation setup adopted for this study. Section 4 contains results of simulations with the drag approach and comparisons with measurements and simulations using the original version of TEB. Section 5 provides conclusions and implications for future work.

2. Inclusion of a drag approach in TEB

Lemonsu et al.'s (2004) single-layer version of TEB (here referred to as TEB_REF) simulates the exchanges between the surface and atmospheric forcing level using an aerodynamical resistances network. In the present version of TEB (here referred to as TEB_SBL), several prognostic air layers are added within and above urban canopy, up to the forcing level. That way, the single-layer version of TEB will gain by

the explicit physical representation of surface boundary layer thanks to additional air layers, and still be coupled to MMMs through only one layer (see Masson and Seity 2008, manuscript submitted to *J. Appl. Meteor. Climatol.* for more details). Thus, with TEB_SBL the exchanges with SBL air occur at ground level and at the SBL scheme levels in contact with buildings. So, to improve the computation of meteorological fields inside the urban canopy, drag force approach that was used for vegetation canopy (Yamada 1982) and has been recently extended to urban canopy (Brown and Williams 1998; Martilli et al. 2002; Dupont et al. 2004; Otte et al. 2004; Hamdi 2005) is applied in this study to represent thermal and dynamical effects of buildings.

a. Dynamical effect

By applying the drag approach, momentum and TKE equations of TEB_SBL are modified to account for the area-average effect of the subgrid urban elements:

$$\frac{\partial U}{\partial t} = F_U + \frac{\partial U}{\partial t}\bigg|_{\text{TEB}} \quad \text{and} \quad (1)$$

$$\frac{\partial k}{\partial t} = F_k + \frac{\partial k}{\partial t}\bigg|_{\text{TEB}}, \quad (2)$$

where U is wind speed, k is the TKE, F_U and F_k are the general forcing terms in each equation (Masson and Seity 2008, manuscript submitted to *J. Appl. Meteor. Climatol.*), and $\partial U/\partial t|_{\text{TEB}}$ and $\partial k/\partial t|_{\text{TEB}}$ are the terms induced by interaction between solid surfaces and airflow.

1) MOMENTUM

The $\partial U/\partial t|_{\text{TEB}}$ term can be partitioned into (i) $\partial U/\partial t|_{\text{TEB}}^V$, the contribution of vertical surfaces (building walls), and (ii) $\partial U/\partial t|_{\text{TEB}}^H$, the contribution of horizontal surfaces (roads and roofs) as it is done in Martilli et al. (2002):

$$\frac{\partial U}{\partial t}\bigg|_{\text{TEB}} = \frac{\partial U}{\partial t}\bigg|_{\text{TEB}}^V + \frac{\partial U}{\partial t}\bigg|_{\text{TEB}}^H. \quad (3)$$

Exchanges of momentum at the vertical surface interface are parameterized as the effect of pressure and drag forces induced by buildings:

$$\frac{\partial U}{\partial t}\bigg|_{\text{TEB}}^V = -C_D\left(\frac{S_V}{V_{\text{air}}}\right)U^2, \quad (4)$$

where C_D is the canopy drag coefficient. For simplicity, C_D is assumed to be constant in the vertical direction and set to 0.4 for all urban areas (Martilli et al. 2002). Here, (S_V/V_{air}) is the vertical surface area of buildings (wall) per unit volume of air in the urban grid cell,

expressed in meters squared per meter cubed. Note that air is assumed to occupy all space of the urban grid cell as when there are no buildings.

The presence of horizontal surfaces like roads, roofs, or canyon floors introduces a frictional force with consequent loss of momentum. This term is similar to that usually present in MMM to represent the impact of the ground surface. The Monin–Obukhov approach for a constant flux layer is assumed in the absence of an alternative theory:

$$\left.\frac{\partial U}{\partial t}\right|_{\mathrm{TEB}}^{H} = -U_*^2\left(\frac{S_H}{V_{\mathrm{air}}}\right), \tag{5}$$

where U_* is the friction velocity and S_H is the horizontal surface area of roads and roofs.

2) TURBULENT KINETIC ENERGY

Analogous with what is done in many vegetation canopy models, the extra source term for k has the dimension of a flux and is parameterized as

$$\left.\frac{\partial k}{\partial t}\right|_{\mathrm{TEB}} = C_D\left(\frac{S_V}{V_{\mathrm{air}}}\right)U^3, \tag{6}$$

which generates far more k from mean flow kinetic energy.

3) MIXING LENGTH

We note that the large eddies above urban canopy break when they come in contact with the urban structures, thus creating different turbulence mixing length scales l_m within and above the street canyon. A simple way to do this is (i) to assume that the mixing length is constant within the canopy (Belcher et al. 2003) $l_m = z_H$ (with z_H representing the typical local height of buildings), to reflect the mixing layer turbulence that develops at the top of a fine canopy (Coceal and Belcher 2005), and (ii) to assume a linear variation of the turbulence mixing length scale above the canopy (Macdonald 2000):

$$l_m = z_H \quad \text{if} \quad z < z_H,$$

$$l_m = z_H + \frac{z - z_H}{z_{\mathrm{top}} - z_H}[l_m(z_{\mathrm{top}}) - z_H] \quad \text{if} \quad z \geq z_H, \tag{7}$$

where z_{top} and $l_m(z_{\mathrm{top}})$ are the height and mixing length at the top of the urban canopy layer.

b. Thermal effect

The effect of urban environment on the thermodynamics is captured in TEB_SBL using simplified approximations in air temperature and specific humidity tendency equations:

$$\frac{\partial T}{\partial t} = F_T + \left.\frac{\partial T}{\partial t}\right|_{\mathrm{TEB}} \quad \text{and} \tag{8}$$

$$\frac{\partial q}{\partial t} = F_q + \left.\frac{\partial q}{\partial t}\right|_{\mathrm{TEB}}, \tag{9}$$

where T is the temperature, q is the specific humidity, F_T and F_q are the general forcing terms in each equation (Masson and Seity 2008, manuscript submitted to *J. Appl. Meteor. Climatol.*), and $\partial T/\partial t|_{\mathrm{TEB}}$ and $\partial q/\partial t|_{\mathrm{TEB}}$, are thermal terms induced by interaction with urban structures calculated as

$$\left.\frac{\partial T}{\partial t}\right|_{\mathrm{TEB}} = \frac{(Q_H^{\mathrm{roof}} + Q_H^{\mathrm{road}})}{\rho C_p}\left(\frac{S_H}{V_{\mathrm{air}}}\right) + \frac{Q_H^{\mathrm{wall}}}{\rho C_p}\left(\frac{S_V}{V_{\mathrm{air}}}\right) \tag{10}$$

and

$$\left.\frac{\partial q}{\partial t}\right|_{\mathrm{TEB}} = \frac{(Q_E^{\mathrm{roof}} + Q_E^{\mathrm{road}})}{\rho}\left(\frac{S_H}{V_{\mathrm{air}}}\right), \tag{11}$$

where ρ is the air density, C_p is the heat capacity of dry air, and Q_H and Q_E are the heat and water vapor turbulent fluxes, respectively, calculated between roof/road/wall and atmosphere. In TEB_SBL, $\partial T/\partial t|_{\mathrm{TEB}}$ and $\partial q/\partial t|_{\mathrm{TEB}}$ are added at each atmospheric level in contact with buildings but only one surface energy balance per wall is resolved (with no vertical description of the wall itself). Thus, the calculation of turbulent fluxes is not required at each atmospheric level inside the urban canopy. Contrary to TEB_REF, with the TEB_SBL version wind and temperature of the air inside the canyon are computed in a prognostic manner. This allows a finer forcing of each surface by the air characteristics. The air level at midheight of the canyon, $z_H/2$, is used to compute turbulent fluxes for walls. The lowest SBL level ($z_I = 3$ m in this study) is used for roads, and the first SBL level above canopy top ($z_k = 16$ m in this study) is used for roofs:

$$Q_H^{\mathrm{wall}} = \rho C_p \frac{T_{\mathrm{wall}} - T(z_H/2)}{\mathrm{RES}_{\mathrm{wall}}}, \tag{12}$$

$$Q_H^{\mathrm{roof}} = \rho C_p \frac{T_{\mathrm{roof}} - T(z_k)}{\mathrm{RES}_{\mathrm{roof}}}, \tag{13}$$

$$Q_H^{\mathrm{road}} = \rho C_p \frac{T_{\mathrm{road}} - T(z_1)}{\mathrm{RES}_{\mathrm{road}}}, \tag{14}$$

$$Q_E^{\mathrm{road}} = \rho \frac{q_{\mathrm{sat}}(T_{\mathrm{road}}, p_s) - q(z_1)}{\mathrm{RES}_{\mathrm{road}}}, \quad \text{and} \tag{15}$$

$$Q_E^{\mathrm{roof}} = \rho \frac{q_{\mathrm{sat}}(T_{\mathrm{roof}}, p_s) - q(z_k)}{\mathrm{RES}_{\mathrm{roof}}}, \tag{16}$$

where p_s is the surface pressure, T_i is the surface temperature, and RES_i is the aerodynamic resistance be-

TABLE 1. Measured data from the Basel-Sperrstrasse tower used for the comparison with model results.

Parameter	Instrumentation	Height (m)
Absolute humidity	Psychrometer Pt100	2.6, 13.9, 17.5, 21.5, 25.5, 26.0, 31.7
Air temperature	Psychrometer Pt100	2.6, 13.9, 17.5, 21.5, 25.5, 26.0, 31.7
Longwave downward/upward radiation	Pyrgeometer (CNR1)	31.5
Shortwave downward/upward radiation	Pyranometer (CNR1)	31.5
Net radiation	Pyradiometer (CNR1)	31.5
Sensible heat flux	Ultrasonic anemometer	31.7
Latent heat flux	Ultrasonic anemometer	31.7
Wind u component	Ultrasonic anemometer (R2/USA-1)	3.6, 11.3, 14.7, 17.9, 22.4, 31.7 (at A, B, C, D, E, F; see Fig. 2b)
Wind v component	Ultrasonic anemometer (R2/USA-1)	3.6, 11.3, 14.7, 17.9, 22.4, 31.7
Wind velocity (horizontal, scalar mean)	Ultrasonic anemometer (R2/USA-1)	3.6, 11.3, 14.7, 17.9, 22.4, 31.7
Wind direction	Ultrasonic anemometer (R2/USA-1)	3.6, 11.3, 14.7, 17.9, 22.4, 31.7
Turbulence $w'u'$	Ultrasonic anemometer (R2/USA-1)	3.6, 11.3, 14.7, 17.9, 22.4, 31.7
Turbulence $w'v'$	Ultrasonic anemometer (R2/USA-1)	3.6, 11.3, 14.7, 17.9, 22.4, 31.7
Turbulence $w't'$	Ultrasonic anemometer (R2/USA-1)	3.6, 11.3, 14.7, 17.9, 22.4, 31.7

tween the canyon surfaces and air inside the canyon computed following Lemonsu et al. (2004).

3. Simulation

a. Measurement site

As a part of the Basel urban boundary layer experiment (BUBBLE) measurements in 2001–02 carried out in the city of Basel, a micrometeorological tower was operated in dense urban areas for 9 months: Basel-Sperrstrasse. This site is located in a heavily built-up part of the city. Measurement setup consists of a tower inside a street canyon reaching up to 32 m above ground level (AGL), that is, a little more than 2 times the local building height ($2.2z_H$), instrumented with six ultrasonic anemometer–thermometers and full radiation component measurements. The instruments installed at the highest level were mounted sufficiently far above the surface to ensure that the measurements are representative of the local scale.

Instrumentation was heavily extended during the intense observational period (IOP) between 15 June and 15 July 2002, with additional measurements of turbulent fluxes. In Table 1, we present a brief overview of the observation methods used to gather data appropriate to the comparison with model results. More complete details are available in Rotach et al. (2005) and Christen (2005).

b. Characterization of Basel's city center

The main urban experimental site in the BUBBLE campaign, Basel-Sperrstrasse, is located in a heavily built-up part of the city center (Fig. 1). The station surrounding it is characterized by a dense urban area with residential row houses, enclosing a large inner courtyard. The backyards are either open (green spaces) or built-up by one-story garages, parking lots, and commercial–industrial buildings. The neighborhood has a high plan aspect ratio of buildings and a small plan aspect ratio of vegetation. The shape of roofs is a mixture of the intense observational period approximately 50% flat and 50% pitched roofs. Table 2 gives an overview on the 3D morphometric parameters for buildings and streets (shape and physical properties) used in the present study.

c. The 1D configuration

In this study, TEB_SBL is run offline on a vertical column (SBL levels are chosen at 3, 4, 6, 10, 12, 14, 16, 20, and 25 m AGL) using measurements recorded at the tower top (31.7 m AGL; see Table 1) as the forcing. The integration time step is 300 s. TEB_SBL calculates the meteorological variables from this forcing level down to the ground (Fig. 2). The surface energy balance for the fraction of vegetation contained in Basel's city center is calculated using the ISBA scheme (Noilhan and Planton 1989). Forcing is applied with a 600-s time step to wind, temperature, humidity, and downward global short- and longwave radiation. The period of simulations extends from 16 to 30 June 2002 (15 days in the first half of the IOP). Both TEB_SBL and TEB_REF versions are run to study the impact of modifications and the results are compared with measurements from the tower.

4. Results and discussion

a. Wind speed

The profiles in Fig. 3 show the wind speed normalized by its forcing value at tower top $u/u(z_{for})$. Profiles are averaged using 600-s time step data with neutral stability:

FIG. 1. Aerial photo of the urban site Basel-Sperrstrasse. (Photo copyright by the Swiss Federal Office of Topography.)

$$-0.1 < \frac{z_{\mathrm{for}} - z_d}{L} < + 0.1 \quad \text{and} \quad u(z_{\mathrm{for}}) > 1.0 \text{ m s}^{-1},$$

$$(17)$$

where z_d is the zero-plane displacement height and L is the Monin–Obukhov length. The stability influence on the observed mean wind profile was studied by Christen (2005) over long periods at the same urban site. He shows that normalized gradients in and above the street canyon are strongest during neutral runs and decrease further with increasing instability. And, during seldom-observed stable runs, gradients in the street canyon are the smallest, or even negative, which is due to a com-

plete decoupling of the street canyon air masses during these low-wind situations. Thus, the evaluation of mean wind profile will be restricted in this study to the situations verifying the conditions in Eq. (17).

Results in Fig. 3 show that the observed average profile can be conceptually divided into three layers (Christen 2005). (i) At the bottom there is the *canyon layer*, where winds are greatly reduced resulting from the presence of obstacles. (ii) The *roof layer* around the roof top is characterized by the highest gradients due to the skimming flow over the street canyon. A similarity to profiles measured over and within plant canopies (Finnigan 2000), an upper inflection point, where curva-

TABLE 2. 3D morphometric parameters of Basel-Sperrstrasse for a circle of 250 m around the tower site and the physical properties of urban elements used in the model.

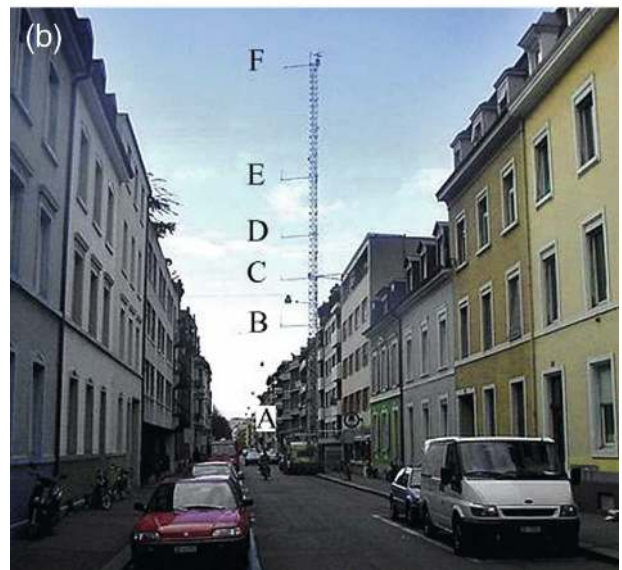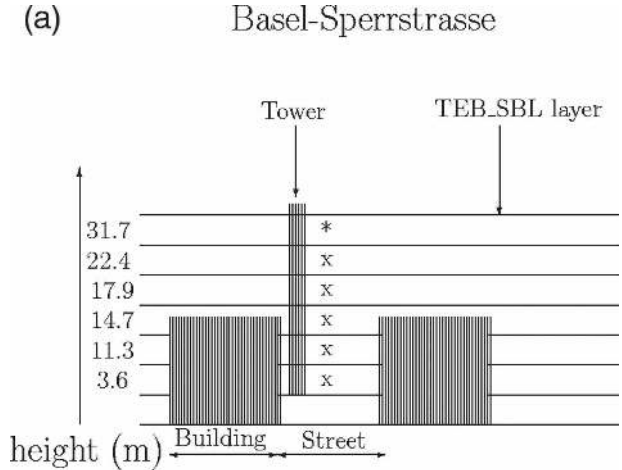| Cover fraction	(Christen 2005)
Vegetation	0.16
Water	0.00
Urban	0.84
Morphometric parameters	(Christen 2005)
Mean building height	14.6 m
Local canyon height to width ratio	1
Plan aspect ratio of buildings	0.54
Frontal aspect ratio of buildings	0.37
Road properties	(Hamdi and Schayes 2005)
Mean materials	Asphalt and concrete over dry soil
Albedo	0.08
Emissivity	0.94
Roughness length for momentum	0.05 m
Roof properties	(Hamdi and Schayes 2005)
Mean materials	45% tiles, 50% gravel, 5% corrugated iron
Albedo	0.14
Emissivity	0.90
Roughness length for momentum	0.15 m
Wall properties	(Hamdi and Schayes 2005)
Mean materials	Plaster, concrete, brick
Albedo	0.14
Emissivity	0.90
Temperature initialization	
Inside building temperature	25°C
Deep soil temperature	17°C

FIG. 2. (a) Configuration of the 1D TEB_SBL, with forcing from the top (*), and calculation down to the ground in the street canyon (x), and schematic representation of the city (street and buildings). (b) The labels in the photo refer to the instrumentation according to Table 1.

ture changes from negative to positive, is found around the canopy top. (iii) Finally, the *above-roof layer* is expected to approximate the well-known log-type profile of the inertial sublayer (Raupach et al. 1991).

The TEB_SBL is able to represent the overall shape of the observed profile. The reason for that arises from the fact that this new canopy parameterization takes into account the repartition of drag force in the momentum equation along the vertical, from the ground up to roof height. The TEB_SBL is able to simulate also the inflection point that appears just above roof level between z_H and $1.2z_H$ (Christen 2005). And, the height of the inflection point is in agreement with observations. However, it appears that simulated drag force is underestimated in the upper part of the street canyon. This is due to the fact that in TEB_SBL, which takes the local characteristics as input, the mean building height is small in comparison with that in some sections of the upwind area of influence. The observations, in turn, are influenced by a fetch that may include

larger, higher, and more complicated structures (the standard deviation of building height inside the 250-m circle around the site is about 6.9 m; Christen 2005).

Figure 4 presents time variation of wind speed from 16 to 19 June (the others days show similar behavior to the observations) at 3.5 and 11.3 m AGL within the street canyon and at 18 m AGL (i.e., above roof level, for TEB_SBL and measurements). In Fig. 4b, we present also the diagnostic 10-m wind speed, calculated with TEB_REF, in which an exponential decay form of the vertical wind profile inside the canyon is assumed.

The TEB_SBL version fits better to the observations at 11.3 m AGL than the diagnostic one, which overestimates wind speed inside the street canyon. This re-
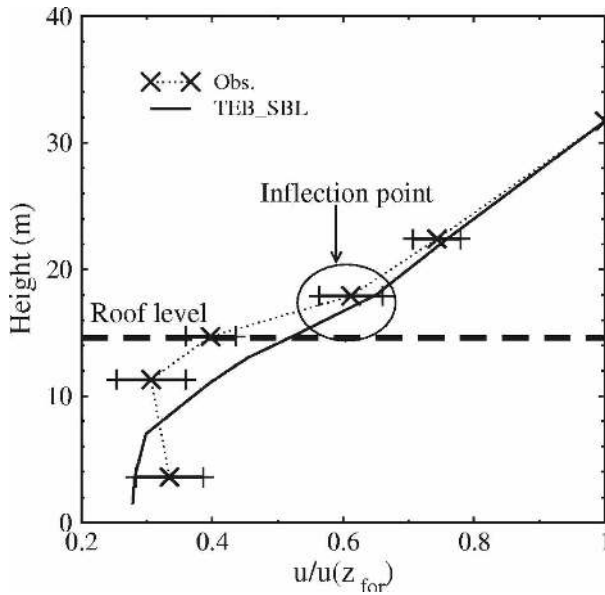
FIG. 3. The average vertical profile of wind speed, normalized by $u(z_{for})$ at the tower top during the first half of the IOP in the frame of BUBBLE, for measurements and TEB_SBL. Data source: Sonic, 600-s time step, neutral stability at tower top, and calm situations with a mean wind speed lower than 1 m s^{-1} at top level are excluded. The bars present the std dev of the observations.

sult agrees with the study of Holt and Pullen (2007), who assess the impact of a single-layer module, based on Kusaka et al. (2001), and a multilayer module, based on Brown and Williams (1998), in a high-resolution mesoscale model applied to the New York City metropolitan area. They found that for the densely urbanized area of Manhattan, winds are generally stronger for the single-layer parameterization than for the multilayer one.

Good correlation is found between observations and TEB_SBL at 3.5 and 18 m AGL. However, one can see from Fig. 4c that TEB_SBL overestimates the wind speed at 18 m AGL during the nights of 17 and 18 June. In fact, when analyzing wind direction at tower top during this episode (see Fig. 5), the direction is mainly perpendicular to the street[1] and the wind blows over pitched roofs (Christen 2005). Generally, flow over pitched roofs results in much lower wind velocities in the street canyon than flow over flat roofs (Christen 2005). As a consequence, vertical exchange is significantly reduced during these conditions. Thus, in TEB_SBL, which takes the local characteristics as an input, the mean building height is small in comparison

_____

[1] The orientation of the street canyon and its perpendicular direction are deduced from a Basel city map and are set, respectively, to 70° and 160°. See Roulet et al. (2005, their Fig. 2).
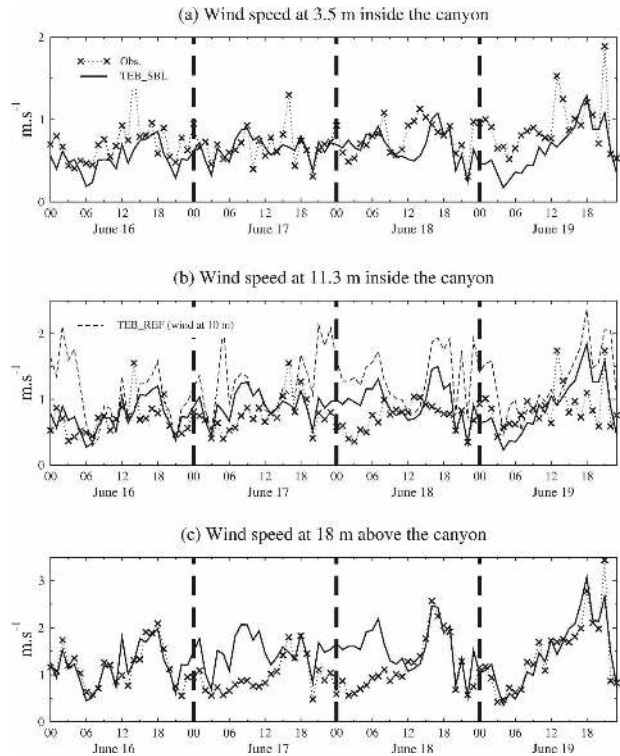

FIG. 4. Time variation of wind speed from 16 to 19 Jun (a) inside the street canyon at 3.5 m AGL, (b) inside the street canyon at 11.3 m AGL, and (c) above the urban canopy at 18 m AGL for measurements and TEB_SBL. In (b), we present also the diagnostic 10-m wind speed calculated with the TEB_REF version.

with that in some sections of the upwind area of influence. A similar pattern can be observed for the nights of 23 and 27 June (not shown).

Roulet et al. (2005) found a similar result with the detailed multilayer urban surface exchange parameterization of Martilli et al. (2002), validated between 25 and 28 June 2002 over the same urban site of Basel-Sperrstrasse. They found that the multilayer urban module overestimates wind speed above roof level on 27 June and that the relative overestimation is even stronger during the night.

b. Temperature

Figure 6 shows the time variation of air temperature from 16 to 19 June (17, 18, and 19 are clear-sky days) at 2.5 and 14 m AGL within the street canyon and at 18 m AGL (i.e., above roof level) for TEB_SBL and measurements. In Figs. 6a and 6b, we present also the diagnostic canyon temperature calculated with TEB_REF, in which canopy temperature is assumed to be constant inside the street canyon.

Near the ground, at 2.5 m AGL, both TEB_SBL and TEB_REF simulations are in good agreement with
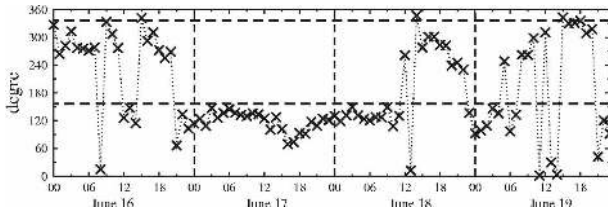
FIG. 5. The wind direction (°) at the tower top at Basel-Sperrstrasse from 16 to 19 Jun. The dashed horizontal lines indicate the directions (160° and 340°) perpendicular to the street canyon.

measurements. The results near roof level, at 14 m AGL, allow some differences to be shown between the two simulations, especially during daytime (the other days of the simulated period show similar behavior; not shown). TEB_REF overestimates canyon temperature during the day. Lemonsu et al. (2004) obtained similar results with TEB validated over Marseilles city center, France. They found that TEB overestimates the canyon temperatures much more during the day. With the new prognostic TEB_SBL version, predictions of temperatures agree much more closely with the observations (see appendix). This result agrees with the study of Holt and Pullen (2007). They found that single-layer parameterization is generally warmer at daytime over much of the metropolitan area by approximately 1°C.

The vertical profile of potential temperature shows similar behavior to the observations for the simulated period. Therefore, in Fig. 7, we present the averaged vertical profile, from 16 to 19 June 2002, of the observed and simulated potential temperature at 0200, 0800, 1600, and 2200 LT. The observed vertical profile of potential temperature at daytime (Figs. 7b,c) shows a pronounced gradient around roof level and small gradient above. TEB_SBL is able to reproduce this shape, but underestimates the temperature inside the street canyon by 0.3°C and computes a gradient that is too large above roof level. TEB_SBL calculates heat fluxes from the street, roof, and walls. Heat sources are then distributed along the vertical up to roof level. The nocturnal urban canopy computed with TEB_SBL (Figs. 7a,d) shows a slightly unstable layer that is in agreement with the results of the detailed multilayer urban surface exchange parameterization of Martilli et al. (2002), found in Hamdi and Schayes (2005) and Roulet et al. (2005), but underestimates the temperature inside the street canyon by 0.5°C.

c. Momentum exchange

A main characteristic of the urban roughness sublayer is a profile of turbulent momentum transport, which is not constant with height (Rotach 1999). For an assessment of the influence of TEB_SBL on the turbulent
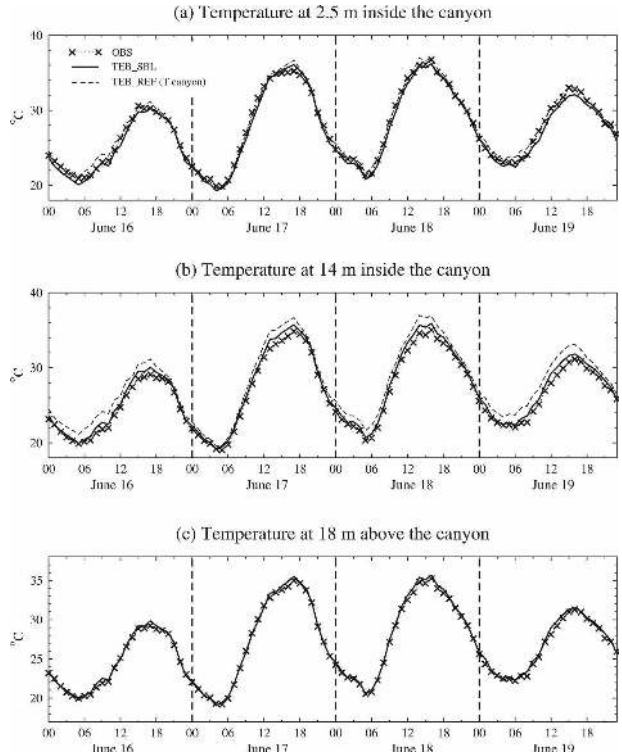

FIG. 6. Time variation of air temperature from 16 to 19 Jun (17, 18, and 19 are clear-sky days) at (a) 2.5 and (b) 14 m AGL, respectively, within the street canyon, and (c) at 18 m AGL (i.e., above roof level) for TEB_SBL and measurements. In (a) and (b), we present also the diagnostic canyon temperature calculated with the TEB_REF version.

exchange of momentum, it will be of interest to look at the local friction velocity defined as

$$U_*(z) = \left(\overline{w'u'}^2 + \overline{w'v'}^2 \right)^{(1/4)}. \tag{18}$$

The notation $U_*(z)$ denotes the explicitly height-dependent local value in the present study; $\overline{w'u'}$ and $\overline{w'v'}$ represent the turbulent momentum transports as functions of height z. These two terms are measured in the urban canopy (see Table 1) and calculated with the urban canopy parameterization. TEB_SBL has a k–l turbulence closure based on the work of Redelsperger et al. (2001). Hence, above the ground surface the vertical turbulent fluxes are computed using K theory:

$$\overline{w'\varphi'} = -K \frac{\partial \overline{\varphi}}{\partial z}, \tag{19}$$

where φ stands for any of the scalar variables u, v, or T; $\overline{w'\varphi'}$ represents the fluxes of the given variable; and K is the vertical turbulent diffusion coefficient, calculated as

$$K = C l_m \sqrt{k}, \tag{20}$$
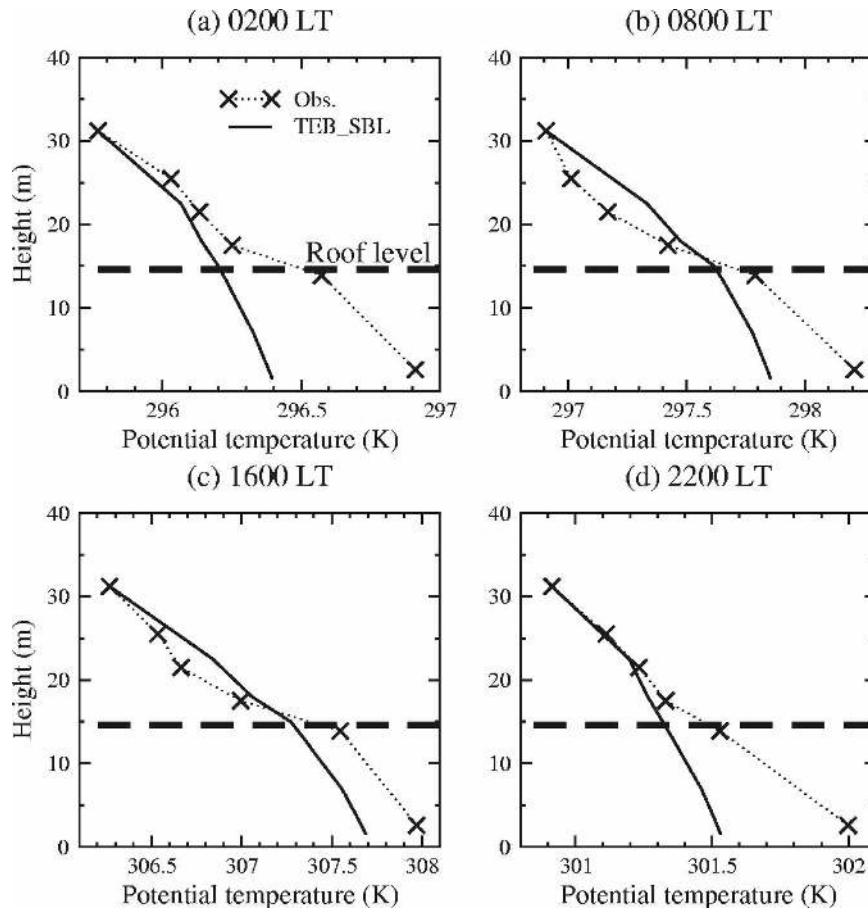
where C is a constant.

FIG. 7. Averaged vertical profile, from 16 to 19 Jun 2002, of the observed and simulated potential temperature in the street canyon at 0200, 0800, 1600, and 2200 LT.

The profiles in Fig. 8 show local friction velocity normalized by its value at tower top $U_*(z_{for})$. Profiles are averaged using 600-s time step data for all stabilities. The observed vertical profile is characterized by a maximum above roof level at $z_f/z_H = 1.5$ and a decrease toward the ground inside the canopy. Above z_f, the average profile is characterized by a slight reduction of U_* to the topmost measurements level. Hence, the region above z_f can be approximated by a constant U_* with height. This is an indication for the transition to the inertial sublayer, as suggested by Rotach (2001) and Kastner-Klein and Rotach (2004). The same behavior has been observed over long periods at the same urban site by Christen et al. (2003) and for other real and modeled wind tunnel canopies (e.g., Rotach 1995; Kastner-Klein et al. 2001; Rotach 2001).

TEB_SBL is able to represent in broad terms the increase of U_* occurring with increasing height inside the urban canopy. But, the value of z_f is somewhat lower (just above roof level) than the one shown by measurements. Taking the same local characteristics of

Basel-Sperrstrasse as used in this study, Hamdi (2005) and Roulet et al. (2005) have difficulties simulating the maximum of friction velocity above roof level with the multilayer urban module of Martilli et al. (2002). This is probably due to the specification of the mixing length in the urban roughness sublayer. However, in Martilli et al. (2002), where the urban canopy layer extends to $z/z_H = 2.4$, using normalized U_* data from Rotach (2001) based on a combination of measurements and wind tunnel studies, U_* is maximized at $z/z_H = 2$ and there is a sharp decrease of U_* toward the ground (as is found in the present study). We hence conclude that the reason for the lower maximum in the present study lies in the specification of the height of buildings since we do not take into account horizontal variability of the height distribution of buildings.

Figure 9 presents time variation of the friction velocity U_* from 16 to 19 June at 3 and 18 m AGL, and at the tower top for TEB_SBL and measurements. In Fig. 9c we present also the friction velocity calculated with TEB_REF. Near the ground (Fig. 9a), TEB_SBL
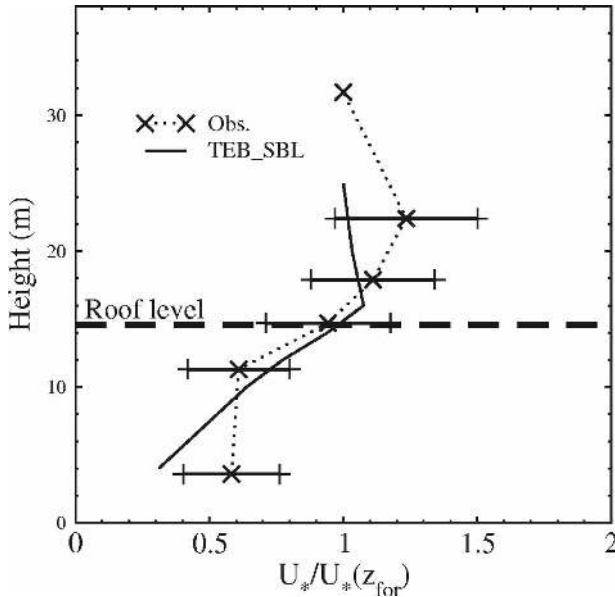
FIG. 8. The average profile of the local friction velocity normalized by its value at tower top $U_*(z_{for})$ for TEB_SBL and measurements. The profiles are averaged using 600-s time step data obtained during the first half of the IOP (15 days) for all stabilities. The bars present the std dev of the observations.

FIG. 9. Time variation of the friction U_* from 16 to 19 Jun in the street canyon at (a) 3 m AGL, (b) 18 m AGL (i.e., above the canyon), and (c) the tower top for TEB_SBL and measurements. In (c) we present also the friction velocity calculated with TEB_REF at tower top.

seems to underestimate the local friction velocity especially during daytime. However, at the tower top (Fig. 9c), TEB_REF has a tendency to overestimate friction velocity during daytime.

d. Turbulent exchange of heat

Figure 10 presents time variation of turbulent heat flux from 16 to 19 June inside the street canyon at 3 m AGL (top) and above roof level at 18 m AGL (bottom) for TEB_SBL and measurements. Near the ground (Fig. 10a), TEB_SBL clearly underestimates vertical heat flux, which is due to the wind speed underestimation inside the street canyon at 3.5 m AGL (see Fig. 4a), but observed values of the fluxes are also very small (<0.05 K m s^{-1}). Above roof level, values calculated by TEB_SBL correspond very well to the measurements. Time series for other days of the simulated episode were similar to those shown here.

Inside street canyon, as well as above roof level, TEB_SBL succeeds in producing a positive turbulent heat flux at night, which produces TKE (Fig. 11) and thus, the nocturnal profile remains neutral and never becomes stable. This phenomenon is mainly driven by the high heat storage release during the night (Hamdi and Schayes 2005, 2007).

Averaged vertical profiles, from 16 to 19 June 2002, of turbulent heat flux at 0200, 0800, 1600, and 2200 LT
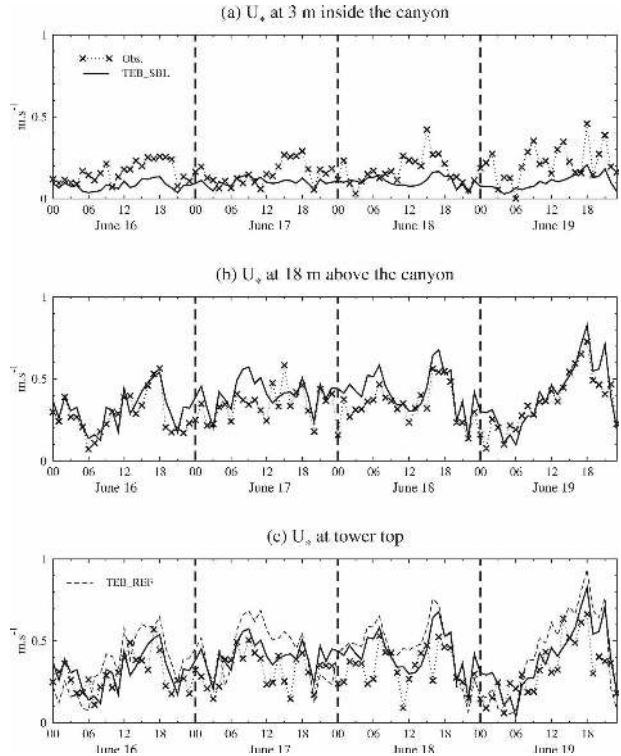
for TEB_SBL and measurements are plotted in Fig. 12. The daytime profiles (Figs. 12b,c) suggest that the strongest gradients are found around the roof top; this feature is well captured by TEB_SBL. The dense urban surface with its narrow street canyon absorbs mainly shortwave radiation in the roof layer and in the upper canopy. As a consequence, sources of heat are strongest in the roof layer. Values that are obtained by TEB_SBL during nighttime (Figs. 12a,d) are, however, much smaller than measurements.

e. Surface energy balance

TEB_SBL is evaluated using measured hourly energy fluxes at the tower top: net radiation Q^*, sensible heat flux Q_H, and latent heat flux Q_E. Sensible and latent heat fluxes are directly derived from eddy correlation measurements using 3D ultrasonic anemometer–thermometers combined with humidity fluctuation measurements, while the heat storage flux ΔQ_S was determined as the residual term.

The daytime/nighttime Q^* is very well reproduced (Fig. 13a). The decrease of Q^* during the morning on

FIG. 10. Time variation of turbulent heat flux $\overline{w'\theta'}$ from 16 to 19 Jun (a) in the street canyon at 3 m AGL and (b) at 18 m AGL (i.e., above the canyon) for TEB_SBL and measurements.
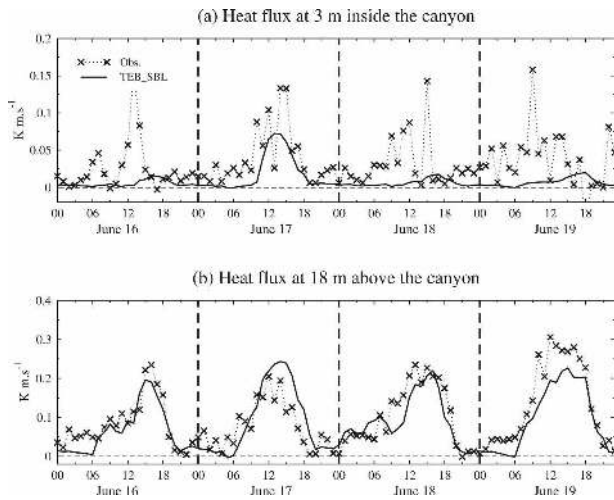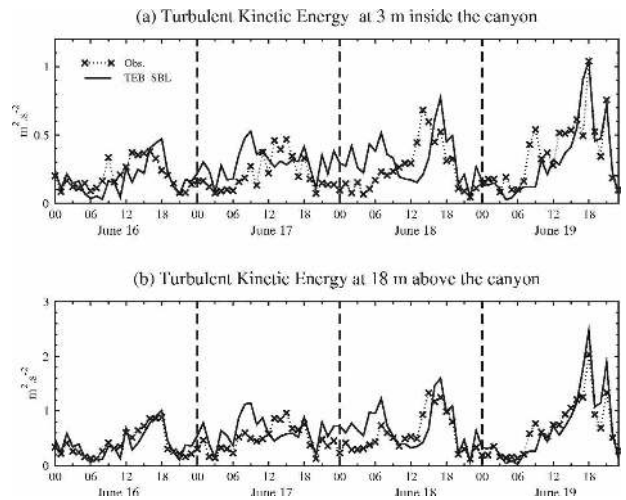

FIG. 11. Time variation of kinetic turbulent energy from 16 to 19 Jun (a) in the street canyon at 3 m AGL and (b) at 18 m AGL (i.e., above the canyon) for TEB_SBL and measurements.
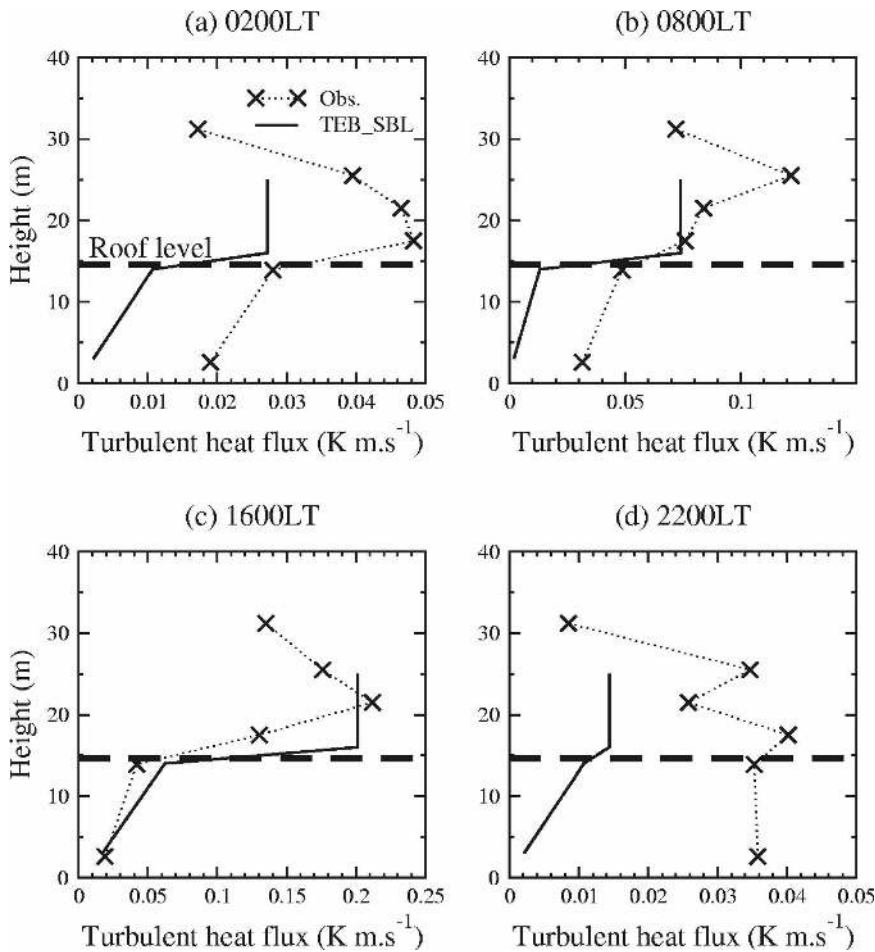

FIG. 12. Averaged vertical profile, from 16 to 19 Jun 2002, of the observed and simulated turbulent heat flux $\overline{w'\theta'}$ in the street canyon at 0200, 0800, 1600, and 2200 LT.
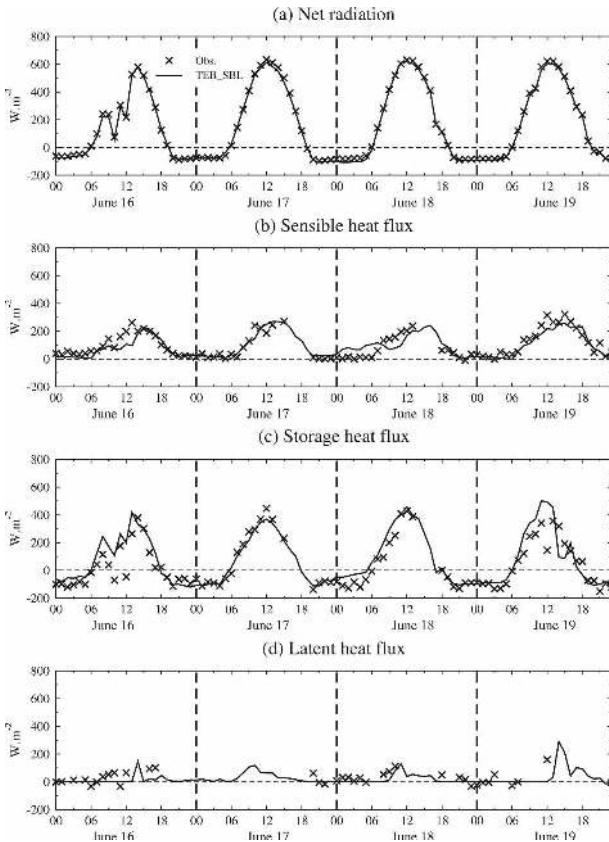
FIG. 13. Comparison between observed and simulated surface energy balance with the TEB_SBL version at the top of the tower.

16 June is the result of a cloud episode over the region. It is easily understandable that the lower the vegetation cover, the less latent heat flux (see Fig. 13d). In fact, in Basel's city center, vegetation cover is small (16%), which limits the degree of evapotranspiration. During the day, the observed Q_H (Fig. 13b) is characteristically around 40% of Q^*. In fact, given the small vegetation cover in the city center, we would like to better understand the energy partitioning between the two sensible heat fluxes, namely, conduction into the underlying buildings and ground ΔQ_S and convection to the air Q_H. During the night, TEB_SBL succeeds in producing a positive sensible heat flux. The observed ΔQ_S (Fig. 13c) increases more rapidly during the morning than Q_H and peaks earlier, whereas the sensible heat flux almost reaches its maximum in the afternoon. During the afternoon, ΔQ_S becomes negative and releases energy to the surface 1 or 2 h before the net radiation becomes negative. The huge daytime ΔQ_S into buildings is counterbalanced by an extremely high nocturnal release of ΔQ_S, which can be even higher in magnitude than the radiative loss. This imbalance maintains an average upward-directed Q_H. Thus in summary, the

TEB_SBL version is able to reproduce correctly most of the behavior of the fluxes typical of the city center of Basel, including the large heat uptake by the urban fabric and the positive Q_H at night.

f. Summary of the results

As a summary for the evaluation of the new version of TEB, bias and root-mean-square error (rmse) over seven clear-sky days (17, 18, 19, 22, 23, 29, and 30 June) between TEB_SBL and measurements on one hand, and between TEB_REF and measurements on the other hand, are calculated in Tables 3 and 4. The root-mean-square errors are clearly lower for TEB_SBL than for TEB_REF for all variables that are presented in Table 3, and this is more pronounced inside the street canyon for wind speed and temperature. TEB_SBL better simulates wind speed inside the street canyon with a bias of 0.11 m s^{-1} and an rmse of 0.33 m s^{-1} for the overall period, while TEB_REF overestimates the wind speed with a bias of 0.39 m s^{-1} and an rmse of 0.57 m s^{-1} during daytime, and this overestimation is more pronounced during the night: 0.66 and 0.77 m s^{-1} for bias and rmse, respectively. For the air temperature at 2.5 m AGL (i.e., inside the street canyon), TEB_REF is slightly better during nighttime with a bias of 0.02°C and an rmse of 0.36°C against −0.35° and 0.45°C for TEB_SBL. However, at 14 m AGL (i.e., inside the street canyon), TEB_REF overestimates the air temperature especially during daytime with a bias of 1.90°C and an rmse of 1.97°C, while TEB_SBL is better with 0.82° and 0.89°C for bias and rmse, respectively. Even with the new formulation of the canyon resistance introduced by Lemonsu et al. (2004), TEB_REF did not produce sufficiently rapid ventilation of the heat released by the urban surfaces inside the canyons. For the friction velocity above the street canyon, TEB_REF overestimates the observations during daytime by 0.15 m s^{-1} against 0.04 m s^{-1} for TEB_SBL.

Table 4 compares observed and simulated shortwave and longwave radiation $S\uparrow$ and $L\uparrow$, respectively. The incoming shortwave and longwave radiation is used as inputs. For both types of outgoing radiation, the TEB_REF and TEB_SBL versions are very close to observations. Rmse values of $L\uparrow$ for the overall period are 12 and 16 W m^{-2}, respectively, and the rmse value of $S\uparrow$ is 4 W m^{-2} for the two versions of TEB. However, the nighttime/daytime bias and rmse comparison shows that the outgoing longwave radiation seems slightly underestimated by TEB_SBL, probably because of low simulated average surface temperatures, $T_{\text{road}}(\text{REF}) - T_{\text{road}}(\text{SBL}) \approx 3°C$ and $T_{\text{wall}}(\text{REF}) - T_{\text{wall}}(\text{SBL}) \approx 1°C$ (the roof temperatures are the same for the two ver-

TABLE 3. Performance statistics for wind (U), temperature (T), and local friction velocity (U_*) between TEB_SBL and measurements and between TEB_REF and measurements over seven clear-sky days (17, 18, 19, 22, 23, 29, and 30 Jun). Obs, SBL, and REF refer to the mean values; Bias = SBL (REF) − Obs; T, D, and N refer to the overall, daytime, and nighttime periods, respectively. In Tables 3, 4, and 5, the boldface values are the most important values on which one should focus.

Level (m)		U (m s^{-1})			T (°C)			U_* (m s^{-1})		
		3	11.3	18	2.5	14	18	3	18	31.5
Obs	T	0.86	0.83	1.32	24.87	23.63	23.80	0.19	0.37	0.35
	D	0.96	0.94	1.54	26.64	25.13	25.34	0.23	0.43	0.41
	N	0.73	0.68	1.03	22.54	21.67	21.79	0.14	0.28	0.27
SBL	T	0.67	0.94	1.54	24.52	24.25	24.04	0.11	0.42	0.42
	D	0.75	1.05	1.72	26.30	25.96	25.69	0.12	0.47	0.47
	N	0.56	0.78	1.29	22.19	22.00	21.89	0.08	0.35	0.35
REF	T	—	1.31	—	25.09	25.09	—	—	0.47	0.47
	D	—	1.29	—	27.03	27.03	—	—	0.58	0.58
	N	—	1.35	—	22.56	22.56	—	—	0.31	0.31
Bias-SBL	T	−0.19	**0.11**	0.22	−0.35	**0.61**	0.24	−0.08	**0.05**	0.07
	D	−0.21	**0.11**	0.18	−0.34	**0.82**	0.35	−0.11	**0.04**	0.06
	N	−0.17	**0.10**	0.26	−0.35	**0.33**	0.10	−0.06	**0.07**	0.08
Bias-REF	T	—	**0.48**	—	0.23	**1.46**	—	—	**0.10**	0.12
	D	—	**0.39**	—	0.38	**1.90**	—	—	**0.15**	0.17
	N	—	**0.66**	—	0.02	**0.88**	—	—	**0.03**	0.04
Rmse-SBL	T	0.30	0.33	0.46	0.56	0.71	0.36	0.12	0.10	0.14
	D	0.32	0.34	0.42	0.63	0.89	0.44	0.15	0.09	0.13
	N	0.28	0.31	0.50	0.45	0.37	0.20	0.08	0.12	0.14
Rmse-REF	T	—	0.67	—	0.49	1.60	—	—	0.16	0.19
	D	—	0.57	—	0.57	1.97	—	—	0.17	0.21
	N	—	0.77	—	0.36	0.93	—	—	0.14	0.15

sions of TEB). Nevertheless, the comparison between the simulated and observed net radiation confirms that TEB_REF and TEB_SBL simulate accurately the net radiation balance.

TABLE 4. As in Table 3, but for outgoing solar ($S\uparrow$) and longwave ($L\uparrow$) radiation, and surface energy balance fluxes recorded at the top of the tower (W m^{-2}). The symbol // means that TEB_REF and TEB_SBL have the same values.

		$S\uparrow$	$L\uparrow$	Q^*	Q_H	ΔQ_S
Obs	T	34	467	179	112	24
	D	57	494	373	189	143
	N	4	431	−76	26	−111
SBL	T	31	453	170	103	47
	D	55	483	358	172	170
	N	1	415	−81	26	−92
REF	T	//	462	160	137	11
	D	//	492	349	219	116
	N	//	421	−88	45	−106
Bias-SBL	T	−3	−14	**−11**	**−9**	**23**
	D	−2	−12	**−15**	**−18**	**27**
	N	−3	−16	**−6**	**1**	**19**
Bias-REF	T	//	−5	**−19**	**25**	**−12**
	D	//	−2	**−24**	**30**	**−27**
	N	//	−10	**−12**	**19**	**5**
RMSE-SBL	T	4	16	29	49	70
	D	5	15	37	60	91
	N	3	17	10	31	35
RMSE-REF	T	//	12	34	56	64
	D	//	10	42	64	83
	N	//	13	17	44	30

The comparison between simulated and observed Q_H shows that the bias is clearly lower for TEB_SBL with a value of −9 W m^{-2} for the overall period against 25 W m^{-2} for TEB_REF. In fact, TEB_REF overestimates the wind speed inside the street canyon and thus produces higher values of Q_H. This result agrees with the study of Holt and Pullen (2007). They found that values of Q_H for multilayer parameterization are less than single-layer parameterization both at daytime (approximately 150 versus 200 W m^{-2}) and nighttime (approximately 10 versus 15 W m^{-2}). The observed ΔQ_S are a residual term in the energy balance, and they accumulate the errors of the other heat fluxes. In TEB_REF and TEB_SBL simulations, average ΔQ_S behaves well like the flux deduced from the observations. The overall rmse is equal to 64 and 70 W m^{-2}, respectively. It appears that the overestimation (underestimation) of Q_H by the TEB_REF (TEB_SBL) is compensated for by ΔQ_S underestimation (overestimation).

g. Sensitivity study to urban canopy representation

The ability of the TEB_SBL to better reproduce meteorological field inside the street canyon, and most features of surface–atmosphere energy exchanges, has been demonstrated. However, to use this urban parameterization in an operational model, many input pa-

TABLE 5. Sensitivity analysis of the rmse to varying input geometric parameters for TEB, relative to the reference case presented in Table 2: RMSE − RMSE (ref).

		U (m s^{-1}) at 11.3 m		T (°C) at 14 m		U_* (m s^{-1}) at 18 m	
		SBL	REF	SBL	REF	SBL	REF
Building fraction + 0.20	D	0	−0.04	−0.01	0	0	+0.03
	N	+0.01	+0.02	**-0.04**	**+0.14**	0	+0.01
Building fraction − 0.20	D	0	+0.06	−0.07	−0.02	−0.01	−0.02
	N	0	−0.05	**−0.03**	**−0.06**	−0.01	−0.01
Building height − 10 m ($\sim z_H/2$)	D	**+0.72**	**−0.02**	**−0.25**	**−0.07**	**+0.01**	**+0.01**
	N	**+0.56**	**−0.03**	**−0.11**	**−0.03**	**−0.03**	**0**
Wall/plane area ratio + 0.20	D	−0.03	0	−0.05	−0.01	+0.01	0
	N	−0.02	+0.01	**−0.03**	**+0.07**	+0.01	0
Wall/plane area ratio − 0.20	D	+0.10	0	−0.01	0	−0.01	0
	N	+0.05	0	**−0.04**	**−0.08**	−0.02	0

rameters are subject to uncertainties. Therefore, in this last section, we will study the sensitivity of the two versions of TEB (SBL and REF) to the specification of the urban morphology via dedicated runs across a range of values for some geometric parameters. Table 5 lists the modifications and the resulting sensitivity of the rmse to (i) wind speed and (ii) air temperature inside the canyon; and (iii) the friction velocity above roof level. Comparisons are made against the reference case presented in the previous section (see Table 2). Results in Table 5 show that an error of a factor of 2 in assigning building height has a larger impact in the TEB_SBL version for the fine description of the air characteristic profiles than in TEB_REF for the mean canyon air ones. This is due to the fact that the comparison is made against the observations at 11.3 m AGL, which are inside the canyon in the TEB_SBL standard simulation and above the canopy in the sensitivity simulation. For the building fraction and the wall/plane area ratio, the TEB_REF seems to be more sensitive than TEB_SBL, especially for the canyon temperature at night. One should note that the sensitivity on the radiative and turbulent fluxes is the same in TEB_REF and TEB_SBL (not shown).

Another sensitivity study can be done by simulating other city sites. This is presented in the appendix for the sites where TEB has already been validated [Mexico City, Mexico, Vancouver, Canada (Masson et al. 2002), and Marseilles (Lemonsu et al. 2004)]. The radiative and turbulent fluxes are not significantly modified by the inclusion of the SBL scheme. This indicates that the energy balance remains well simulated with TEB_SBL. Furthermore, on the site of Marseilles, a measurement station of temperature and humidity was located in the canyon, and TEB_SBL improves the simulations of the canyon air characteristics.

5. Conclusions and perspectives

Previous offline evaluations of TEB have been conducted against measured fluxes, surface temperatures, and canyon temperature values for three sites under dry conditions: the downtown city center of Mexico City, a light industrial site in Vancouver (Masson et al. 2002), and the downtown core of Marseilles (Lemonsu et al. 2004). Comparisons with field observations show that TEB is able to successfully simulate the behavior of roads, walls, and rooftop temperatures and to correctly partition the radiation forcing into turbulent and heat storage fluxes. However, since TEB is a single-layer module, the characteristics of the air inside the canyon space must be specified. So, to improve the prediction of the meteorological fields inside the street canyon, a new version has been developed (TEB_SBL). Following the methodology of Masson and Seity (2008, manuscript submitted to *J. Appl. Meteor. Climatol.*), it resolves the surface boundary layer (SBL) inside and above the urban canopy by introducing a drag force approach to account for the vertical effects of the buildings. TEB_SBL is tested offline in a street canyon. Results are compared with simulations using the single-layer (Lemonsu et al. 2004) version of TEB (TEB_REF) on the one hand and with measurements inside and above the street canyon on the other hand. The results of the comparison are summarized below.

a. Wind speed

TEB_SBL is able to represent the overall shape of the observed wind speed profile inside the street canyon. It is able to simulate also the inflection point that appears just above roof level, and fits better to the observations at 11.3 m AGL than TEB_REF, which overestimates the wind speed inside the street canyon. However, it appears that the simulated drag force is

underestimated in the upper part of the street canyon, which is due to the fact that in TEB_SBL, the mean building height is small in comparison with that in some sections of the upwind area of influence. The observations, in turn, are influenced by a fetch that may include larger, higher, and more complicated structures.

b. Canyon temperature

Near the ground, both TEB_SBL and TEB_REF versions are in good agreement with measurements. The results near roof level indicate that during daytime, TEB_SBL performs better than TEB_REF, which tends to overestimate the canyon temperature. The observed vertical profile of potential temperature at daytime shows a pronounced gradient around roof level and small gradient above. TEB_SBL is able to reproduce this shape, but underestimates the temperature inside the street canyon by 0.3°C and computes a gradient that is too large above roof level. The nocturnal urban canopy computed with TEB_SBL underestimates the temperature inside the street canyon by 0.5°C.

c. Friction velocity

TEB_SBL is able to represent in broad terms the increase of the local friction velocity occurring with increasing height inside the urban canopy. But, the level of the maximum value is somewhat lower than the one shown by measurements. In our configuration, we do not take into account the horizontal variability of the height distribution of buildings. However, the observations are influenced by a fetch of somewhat larger height variability. The analysis of time series shows that near the ground, although TEB_SBL underestimates the local friction velocity especially during daytime, it fits, in general, better to measurements than does the single-layer version above the canyon.

d. Turbulent exchange of heat

Near the ground, TEB_SBL clearly underestimates the vertical heat flux, but observed values of the fluxes are very small. Above roof level, the values calculated by TEB_SBL correspond very well to the measurements. Inside the street canyon, as well as above roof level, TEB_SBL succeeds in producing a positive turbulent heat flux at night, and thus, the nocturnal profile remains neutral and never becomes stable. Vertical profiles in the street canyon suggest that the strongest gradients are found around the rooftop. This feature is well captured by TEB_SBL.

e. Surface energy balance

The bias of sensible heat flux is clearly lower for TEB_SBL with a value of -9 W m^{-2} for the overall period against 25 W m^{-2} for TEB_REF. In TEB_REF and TEB_SBL simulations the average heat storage flux behaves well like the flux deduced from the observations. The overall rmse is equal to 64 and 70 W m^{-2}, respectively. It appears that the overestimation (underestimation) of sensible heat flux by TEB_REF (TEB_SBL) is compensated for by the storage heat flux underestimation (overestimation).

The surface energy balance is shown to be as well reproduced as on previous sites where TEB_REF was already validated, with better estimation of the meteorological fields inside the street canyon. There is the same sensitivity to urban morphology on energy fluxes as for TEB_REF, and a larger one for canyon air. This is because TEB_SBL is now able to simulate more details, especially the shape of the profiles of wind, temperature, humidity, stress, and heat turbulent flux.

The ability of the method developed in Masson and Seity (2008, manuscript submitted to *J. Appl. Meteor. Climatol.*) to include a fine description of the surface boundary layer into a single-layer urban scheme has been demonstrated here against a heavily observed site in BUBBLE. TEB_SBL stays a single-layer scheme, since it is coupled to the atmosphere (atmospheric model or tower observations) only at one level, located at the top of the SBL scheme. However, it is successful at capturing the structure inside and just above the urban canopy, previously available only when using the complete mesoscale meteorological model coupled to the multilayer urban scheme (as in Martilli et al. 2002). It is also computer efficient, as it does not require small integration time steps while keeping a very high vertical resolution.

Applications are the same as those for classical multilayer schemes. For example, a better description of the turbulence statistics near the surface allows improvement of dispersions studies, or the forcing of chemistry models. But then detailed evaluations of wind speed and turbulence inside the street canyon and across an entire urban region must be done. These issues are beyond the scope of the present article and will be addressed in a subsequent publication. Furthermore, because of the efficiency of the SBL scheme, new research directions can be developed, as in local climatic simulations with the fine description of in-canyon urban climate in the framework of city and global change.

APPENDIX

Application of TEB_SBL to Downtown Marseilles, Downtown Mexico City, and Vancouver Light Industrial Sites

The TEB_SBL was evaluated on the Marseilles city center canyon temperature and energy balance components measured during the field experiments to constrain models of atmospheric pollution and transport of emissions [Experience sur Site pour Contraindre les Modèles de Pollution Atmosphérique et de Transport d'Emissions (ESCOMPTE) urban boundary layer (UBL) campaign between 18 and 30 June 2001 (13 clear-sky days) (description in Lemonsu et al. 2004)].

As shown in Table A1, the TEB_SBL version results in an improvement for the daytime averaged canyon air temperature with a bias of $0.50°$ against $1°C$ for TEB_REF. However, the nocturnal canyon temperature seems to be overestimated by TEB_SBL with a bias of $1.28°$ against $0.95°C$ for TEB_REF. In fact, given the high aspect ratio of the street canyon (1.14), the walls play an important role during the night and the overestimation of the canyon air temperature is apparently due to a too-high emission from the walls, where the surface temperature is overestimated by TEB (see Lemonsu et al. 2004). For the surface energy balance, the TEB_SBL results in no impact for the net

TABLE A2. Variation of heat fluxes between TEB_REF and TEB_SBL for Mexico City and Vancouver light industrial sites ($W \, m^{-2}$).

		$\Delta(Q^*)$	$\Delta(Q_H)$	$\Delta(\Delta Q_S)$
Mexico	D	+1	−7	+8
	N	0	0	−1
Vancouver	D	−1	−7	+7
	N	−1	+1	−2

radiation and an improvement of the sensible heat flux with a nearly removed bias during the day and a smaller rmse.

TEB_SBL was also reevaluated for the downtown area of Mexico City and a light industrial site in Vancouver (see Masson et al. 2002). Table A2 presents the variation of heat fluxes between the two versions of TEB. In both urban sites, the TEB_SBL results in no impact for net radiation and a small decrease in the sensible heat flux ($-7 \, W \, m^{-2}$), which is associated with an increase of the storage heat fluxes ($+7 \, W \, m^{-2}$). With the TEB_SBL version, the bias of heat fluxes is nearly removed during the day.

REFERENCES

Baklanov, A., and Coauthors, 2006: Integrated systems for forecasting urban meteorology, air pollution and population exposure. *Atmos. Chem. Phys.,* **7,** 855–874.

Belcher, S. E., N. Jerram, and J. C. R. Hunt, 2003: Adjustment of the atmospheric boundary layer to a canopy of roughness element. *J. Fluid Mech.,* **488,** 369–398.

Best, M. J., 2005: Representing urban areas within operational numerical weather prediction models. *Bound.-Layer Meteor.,* **114,** 91–109.

——, 2006: Progress towards better weather forecasts for city dwellers: From short range to climate change. *Theor. Appl. Climatol.,* **84,** 47–55.

Brown, M., 2000: Urban parameterizations for mesoscale meteorological models. *Mesoscale Atmospheric Dispersion,* Z. Boybey, Ed., Wesses Press, 193–253.

Brown, M. J., and M. Williams, 1998: An urban canopy parameterization for mesoscale models. Preprints, *Second Symp. on the Urban Environment,* Albuquerque, NM, Amer. Meteor. Soc., 144–147.

Christen, A., 2005: Atmospheric turbulence and surface energy exchange in urban environments. Ph.D. thesis, University of Basel, 130 pp.

——, R. Vogt, and M. W. Rotach, 2003: Profile measurements of selected turbulence characteristics over different urban surfaces. Preprints, *Fourth Int. Conf. on Urban Air Quality,* Prague, Czech Republic, Carolinum University, 408–411.

Cionco, R. M., 1965: A mathematical model for air flow in a vegetative canopy. *J. Appl. Meteor.,* **4,** 517–522.

Coceal, O., and S. E. Belcher, 2005: Mean winds through an inhomogeneous urban canopy. *Bound.-Layer Meteor.,* **115,** 47–68.

Dandou, A., M. Tombrou, E. Akylas, N. Soulakellis, and E. Bossioli, 2005: Development and evaluation of an urban

TABLE A1. Performance statistics for the averaged (for five in-canyon stations in Marseilles city center) canyon temperature at 6 m AGL, and the surface energy balance between TEB_SBL and measurements and between TEB_REF and measurements over 13 clear-sky days between 18 and 30 Jun 2001. Bias = SBL (REF) − Obs.

		Canyon temperature (°C) at 6 m	Q^* ($W \, m^{-2}$) at 37.9 m	Q_H ($W \, m^{-2}$) at 37.9 m	ΔQ_S ($W \, m^{-2}$) at 37.9 m
Bias-SBL	D	0.51	−33	0	2
	N	1.28	−13	−14	9
Bias-REF	D	0.95	−33	4	−1
	N	0.95	−13	−16	11
Rmse-SBL	D	1.10	43	82	94
	N	1.38	17	27	41
Rmse-REF	D	1.30	43	83	95
	N	1.10	17	27	41

parameterization scheme in the Penn State/NCAR Mesoscale Model (MM5). *J. Geophys. Res.,* **110,** D10102, doi:10.1029/2004JD005192.

Dupont, S., and P. G. Mestayer, 2006: Parameterization of the urban energy budget with the submesoscale soil model. *J. Appl. Meteor.,* **45,** 1744–1765.

——, T. L. Otte, and J. K. S. Ching, 2004: Simulation of meteorological fields within and above urban and rural canopies with a mesoscale model (MM5). *Bound.-Layer Meteor.,* **113,** 111–158.

Finnigan, J. J., 2000: Turbulence in plant canopies. *Annu. Rev. Fluid Mech.,* **22,** 519–557.

Grimmond, C. S. B., and T. R. Oke, 1999: Heat storage in urban areas: Local-scale observations and evaluation of a simple model. *J. Appl. Meteor.,* **38,** 922–940.

——, and ——, 2002: Turbulent heat fluxes in urban areas: Observations and a Local-Scale Urban Meteorological Parameterization Scheme (LUMPS). *J. Appl. Meteor.,* **41,** 792–810.

Hamdi, R., 2005: Numerical study of the atmospheric boundary layer over urban areas: Validation for the cities of Basel and Marseilles. Ph.D. thesis, University of Louvain, 42 pp.

——, and G. Schayes, 2005: Validation of the Martilli's urban boundary layer scheme with measurements from two midlatitude European cities. *Atmos. Chem. Phys. Discuss.,* **5,** 4257–4289.

——, and ——, 2007: Sensitivity study of the urban heat island intensity to urban characteristics. *Int. J. Climatol.,* **28,** 973–982.

Holt, T., and J. Pullen, 2007: Urban canopy modeling of the New York City metropolitan area: A comparison and validation of single- and multilayer parameterizations. *Mon. Wea. Rev.,* **135,** 1906–1930.

Kastner-Klein, P., and M. W. Rotach, 2004: Mean flow and turbulence characteristics in an urban roughness sublayer. *Bound.-Layer Meteor.,* **111,** 55–84.

——, E. Fedorovich, and M. W. Rotach, 2001: A wind-tunnel study of organized turbulent motions in urban street canyons. *J. Wind Eng. Ind. Aerod.,* **89,** 849–861.

Kondo, H., and F. H. Liu, 1998: A study on the urban thermal environment obtained through one-dimensional urban canopy model (in Japanese). *J. Japan Soc. Atmos. Environ.,* **33,** 179–192.

Kusaka, H., H. Kondo, Y. Kikegawa, and F. Kimura, 2001: A simple single-layer urban canopy model for atmospheric models: Comparison with multi-layer and slab models. *Bound.-Layer Meteor.,* **101,** 329–358.

Lemonsu, A., and V. Masson, 2002: Simulation of a summer urban breeze over Paris. *Bound.-Layer Meteor.,* **104,** 463–490.

——, C. S. B. Grimmond, and V. Masson, 2004: Modeling the surface energy balance of an old Mediterranean city core. *J. Appl. Meteor.,* **43,** 312–327.

Macdonald, R. W., 2000: Modelling the mean velocity profile within the urban canopy layer. *Bound.-Layer Meteor.,* **97,** 25–45.

Martilli, A., A. Clappier, and M. W. Rotach, 2002: An urban surface exchange parameterization for mesoscale models. *Bound.-Layer Meteor.,* **104,** 261–304.

Masson, V., 2000: A physically-based scheme for the urban energy budget in atmospheric models. *Bound.-Layer Meteor.,* **94,** 357–397.

——, 2006: Urban surface modeling and the meso-scale impact of cities. *Theor. Appl. Climatol.,* **84,** 35–45.

——, C. S. B. Grimmond, and T. R. Oke, 2002: Evaluation of the Town Energy Balance (TEB) scheme with direct measurements from dry districts in two cities. *J. Appl. Meteor.,* **41,** 1011–1026.

Noilhan, J., and S. Planton, 1989: A simple parameterization of land surface processes for meteorological models. *Mon. Wea. Rev.,* **117,** 536–549.

Otte, T. L., A. Lacser, S. Dupont, and J. K. S. Ching, 2004: Implementation of an urban canopy parameterization in a mesoscale meteorological model. *J. Appl. Meteor.,* **43,** 1648–1665.

Piringer, M., and Coauthors, 2007: The surface energy balance and the mixing height in urban areas—activities and recommendations of COST Action 715. *Bound.-Layer Meteor.,* **124,** 3–24.

Raupach, M. R., R. A. Antonia, and S. Rajagopalan, 1991: Roughwall turbulent boundary layers. *Appl. Mech. Rev.,* **44,** 1–25.

Redelsperger, J. L., F. Mahé, and P. Carlotti, 2001: A simple and general subgrid model suitable both for surface layer and free-stream turbulence. *Bound.-Layer Meteor.,* **101,** 375–408.

Rotach, M. W., 1995: Profiles of turbulence statistics in and above an urban street canyon. *Atmos. Environ.,* **13,** 1473–1486.

——, 1999: On the influence of the urban roughness sublayer on turbulence and dispersion. *Atmos. Environ.,* **33,** 401–408.

——, 2001: Simulation of urban-scale dispersion using a Lagrangian stochastic dispersion model. *Bound.-Layer Meteor.,* **99,** 379–410.

——, and Coauthors, 2005: BUBBLE–An urban boundary layer meteorology project. *Theor. Appl. Climatol.,* **81,** 231–261.

Roulet, Y. A., A. Martilli, M. W. Rotach, and A. Clappier, 2005: Validation of an urban surface exchange parameterization for mesoscale models–1D case in a street canyon. *J. Appl. Meteor.,* **44,** 1484–1498.

Vu, T. C., T. Asaeda, and Y. Ashie, 1999: Development of a numerical model for the evaluation of the urban thermal environment. *J. Wind Eng,* **81,** 181–196.

——, Y. Ashie, and T. Asaeda, 2002: A k-ε turbulence closure model for the atmospheric boundary layer including urban canopy. *Bound.-Layer Meteor.,* **102,** 459–490.

Yamada, T., 1982: A numerical model study of turbulent airflow in and above a forest canopy. *J. Meteor. Soc. Japan,* **60,** 439–454.